

Variational Mode Decomposition-Informed Empirical Wavelet Transform for Electric Vibrator Noise Analysis

Zhenyu Xu, Zhangwei Chen

State Key Lab of Fluid Power and Mechatronic Systems, Zhejiang University, Hangzhou, China

Email: 12025049@zju.edu.cn

How to cite this paper: Xu, Z.Y. and Chen, Z.W. (2024) Variational Mode Decomposition-Informed Empirical Wavelet Transform for Electric Vibrator Noise Analysis. *Journal of Applied Mathematics and Physics*, 12, 2320-2332.

<https://doi.org/10.4236/jamp.2024.126138>

Received: May 22, 2024

Accepted: June 25, 2024

Published: June 28, 2024

Abstract

Electric vibrators find wide applications in reliability testing, waveform generation, and vibration simulation, making their noise characteristics a topic of significant interest. While Variational Mode Decomposition (VMD) and Empirical Wavelet Transform (EWT) offer valuable support for studying signal components, they also present certain limitations. This article integrates the strengths of both methods and proposes an enhanced approach that integrates VMD into the frequency band division principle of EWT. Initially, the method decomposes the signal using VMD, determining the mode count based on residuals, and subsequently employs EWT decomposition based on this information. This addresses mode aliasing issues in the original method while capitalizing on VMD's adaptability. Feasibility was confirmed through simulation signals and ultimately applied to noise signals from vibrators. Experimental results demonstrate that the improved method not only resolves EWT frequency band division challenges but also effectively decomposes signal components compared to the VMD method.

Keywords

Electric Vibrator, Noise Analysis, Signal Decomposing, Variational Mode Decomposition, Empirical Wavelet Transform

1. Introduction

The electric vibrator serves as a crucial tool for mechanical environment testing, enabling the generation of controllable waveforms. As the noise signal encapsulates substantial information concerning the operational characteristics of the vibrator, often exhibiting a chaotic nature [1] [2], accurate extraction of signal

features is imperative for analyzing the mechanism and characteristics of noise generation [3].

In recent years, numerous non-stationary signal analysis methods have been introduced. For instance, Potter introduced the short-time Fourier transform in 1947, which elucidates the evolutionary characteristics of signal spectra [4]. Mallat proposed a matching pursuit algorithm based on the projection tracking algorithm, offering considerable flexibility for specific application scenarios [5]. While time-frequency analysis methods have significantly advanced signal decomposition, they predominantly rely on Fourier transform as the foundational theory. Consequently, it often results in contradictory phenomena such as false signals and frequencies. For a more intuitive analysis of non-stationary signals, fundamental quantities and functions with locality are preferred. To address this need, Huang *et al.* introduced the Hilbert Huang transform [6], which, based on the concept of instantaneous frequency, led to the development of the Empirical Mode Decomposition (EMD) method by decomposing any signal into Intrinsic Mode Functions (IMFs) [7]. EMD, being both adaptive and localized, has found wide application despite its inherent drawbacks, such as modal aliasing and endpoint effects.

To optimize EMD, two typical methods have emerged: Variational Mode Decomposition (VMD) and Empirical Wavelet Transform (EWT). VMD, proposed by Dragomiretskiy in 2014, formulates signal decomposition as a variational problem, offering a more solid mathematical foundation [8]. On the other hand, EWT, introduced by Gilles in 2013, integrates the adaptive decomposition concept of EMD with the tightly supported framework of wavelet transform theory, presenting a novel adaptive time-frequency analysis approach for signal processing [9]. While VMD and EWT have been widely applied in various fields, such as earthquake prediction and fault diagnosis, they each possess unique characteristics and limitations [10]-[12]. VMD's mode decomposition is influenced by parameter settings, while EWT requires determination of the number of frequency band division. VMD and EWT are enhanced versions of the EMD algorithm. They can adaptively extract IMFs from non-stationary signals without the need to construct basis functions, making them suitable for decomposing various signals. Due to these capabilities, VMD and EWT share certain similarities, offering theoretical potential for their complementary use. Previous studies have attempted to integrate these two methods [13], yet the high adaptability of VMD mode selection and EWT's effective separation of harmonics with different frequencies in chaotic signals have not been fully exploited. Current research on the integration of these two algorithms lacks a clear framework for optimizing parameter settings. Besides, most approaches rely on empirical and heuristic methods, without systematic theoretical support.

Therefore, this article addresses the similarities and respective shortcomings of the VMD and EWT algorithms by proposing an enhanced approach that integrates VMD into the frequency band division principle of EWT. The validity

of this method is confirmed through simulations and experimental data obtained from the noise signals of an electric vibrator. Consequently, leveraging VMD's adaptability to address EWT's mode number selection problem presents a promising solution.

The method proposed in this article effectively addresses issues such as the lack of adaptive mode selection and mode aliasing during feature extraction from non-stationary signals, as exemplified by electric vibrator noise. This improvement enhances both the efficiency and efficacy of signal decomposition, rendering it of significant application value and engineering importance.

2. Algorithm Derivation

2.1. Variational Mode Decomposition

VMD is a non-recursive decomposition method capable of breaking down a signal into several finite bandwidth components. Assuming the noise signal f , its constrained variational model is depicted in Equation (1).

$$\left\{ \begin{array}{l} \min_{\{u_k\}, \{\omega_k\}} \left\{ \sum_k \left\| \partial_t \left[\left(\delta(t) + \frac{j}{\pi t} \right) * u_k(t) \right] e^{-j\omega_k t} \right\|_2^2 \right\} \\ s.t. \quad \sum_k u_k = f \end{array} \right. \quad (1)$$

where, $\delta(t)$ represents the impulse function, u_k stands for the k -th component obtained through decomposition, and ω_k denotes the center frequency corresponding to u_k . The optimal solution of Equation (1) can be obtained using the augmented Lagrange function, as follows:

$$L(\{u_k\}, \{\omega_k\}, \{\lambda\}) = \alpha \sum_k \left\| \partial_t \left[\left(\delta(t) + \frac{j}{\pi t} \right) * u_k(t) \right] e^{-j\omega_k t} \right\|_2^2 + \left\| f(t) - \sum_k u_k(t) \right\|_2^2 + \left\langle \lambda(t), f(t) - \sum_k u_k(t) \right\rangle \quad (2)$$

where, α represents the quadratic penalty factor, λ denotes the Lagrange parameter. Employing the alternating direction multiplier method to derive the optimal solution of Equation (2), the decomposition component u_k and its corresponding center frequency ω_k are obtained as

$$\hat{u}_k^{n+1} = \frac{f(\hat{\omega}) - \sum_{i \neq k} u_i(\hat{\omega}) + \lambda(\hat{\omega}) / 2}{1 + 2\alpha(\omega - \omega_k)^2} \quad (3)$$

$$\omega_k^{n+1} = \frac{\int_0^\infty \omega |u_k(\hat{\omega})|^2 d\omega}{\int_0^\infty |u_k(\hat{\omega})|^2 d\omega} \quad (4)$$

where, \hat{u}_k^{n+1} is the Wiener filter of $f(\hat{\omega}) - \sum_{i \neq k} u_i(\hat{\omega})$, and ω_k^{n+1} is the center frequency.

2.2. Empirical Wavelet Transform

EWT automatically segments the frequency spectrum of signal f , subsequently

constructing an orthogonal filter bank to decompose f into several components. The detail coefficients of EWT decomposition are calculated as

$$W(n, t) = F^{-1}(\hat{f} \cdot \overline{\hat{\psi}}_n) \quad (5)$$

where, n denotes the n -th frequency band after spectrum segmentation, \hat{f} represents the Fourier transform of f , F^{-1} denotes the inverse Fourier transform; $\overline{\hat{\psi}}_n$ stands for the conjugate of the Fourier transform of wavelet ψ_n .

The approximate coefficients for EWT decomposition is as follows:

$$W(0, t) = F^{-1}(\hat{f} \cdot \overline{\hat{\phi}}_1) \quad (6)$$

where, $\overline{\hat{\phi}}_1$ is the conjugate of the Fourier transform of scaling function ϕ_1 .

The signal reconstruction equation for EWT is

$$f(t) = W(0, t) * \phi_1 + \sum_{n=1}^{N-1} W(n, t) * \psi_n \quad (7)$$

where, $*$ represents the convolution operator. The expression for the decomposition component is as

$$f_0(t) = W(0, t) * \phi_1 \quad (8)$$

$$f_k(t) = W(k, t) * \psi_k \quad (9)$$

2.3. Enhanced Approach

The recursive algorithms like EMD can introduce modal aliasing and endpoint effects, distorting the obtained physical information, while VMD offers improvements in these aspects. However, the preset parameters can significantly impact the center frequency and narrow bandwidth of each mode. Moreover, if both the penalty factor and sampling frequency are incorrectly set, detecting parameter errors becomes challenging due to VMD's high adaptability, despite resulting in problematic decomposition outcomes. Similarly, when using EWT for decomposing noisy signals, reasonable division of signal spectrum boundaries becomes imperative. Only through such division can effective components be separated from noise interference. Essentially, the center frequency and bandwidth of the modes after VMD are influenced by parameter settings. Although EWT can adaptively select bandwidth, determining the number of pattern decompositions remains necessary.

Hence, leveraging VMD's capability to determine the number of modal decompositions based on actual conditions can address the challenge of selecting the number of EWT modes. To tackle these issues, this article proposes an enhanced approach that integrates VMD into the frequency band division principle of EWT, referred to hereinafter as the Enhanced Approach.

Implementation Steps of the Enhanced Approach:

Step 1: Employ VMD to decompose the noise signals and vary the number of modal decompositions. Monitor the residuals, and upon stabilization with a sudden decrease, record the number of modal decompositions at stability as N_s . The EWT frequency band division number is then $N = N_s - 1$.

Step 2: Reconstruct the noise signal decomposed by VMD with a modal number of N , denoted as S .

Step 3: Set the number of frequency bands to N , and utilize EWT to decompose the reconstructed signal S .

3. Approach Performance Analysis

In this section, we will utilize the enhanced approach to analyze harmonic superposition signals, comparing them with VMD to illustrate the superiority of it.

To construct the $f_{sig}(t)$, we can use the following expression:

$$f_{sig}(t) = \cos(8\pi t) + 1/3 \cos(32\pi t) + 1/9 \cos(96\pi t) + n(t) \quad (10)$$

The simulated signal comprises three cosine signals with frequencies of 4 Hz, 16 Hz, and 48 Hz, respectively, alongside white noise with an amplitude of $1/50$ and a power of -20 dB. Sampling points are set to $N = 2000$, and the sampling frequency to $f_s = 1000$ Hz. The waveform of the simulated signal is depicted in the following **Figure 1**.

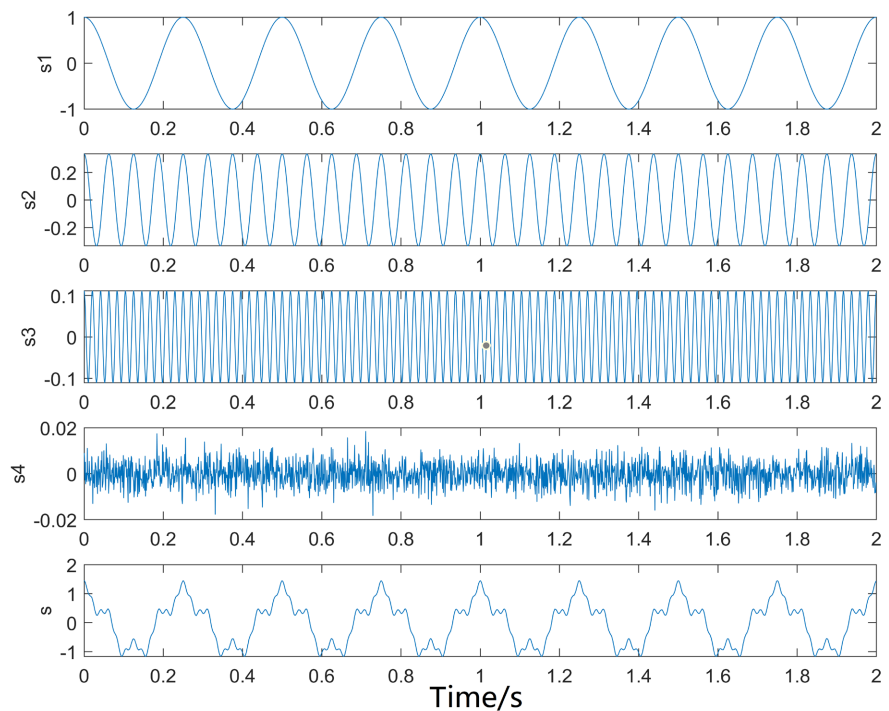


Figure 1. Simulated signal and its components.

Utilizing VMD for signal decomposition, following the principles outlined in section 2.3, we observe that with a modal number set to 4, the peak residual value is 0.0049. Increasing the modal number to 5 yields a peak residual value of 0.0048, while further raising it to 6 results in a sharp drop to 0.0037. Consequently, the mode decomposition number indicating stability is 5. For EWT, the determined mode number by VMD is 4, with the corresponding frequency band division number set to 4.

The decomposition outcomes of the analog signal using VMD and EWT are presented in **Figure 2** and **Figure 3**, respectively. The waveform of each mode component is evident and distinct, allowing clear differentiation of the amplitude and frequency of each mode. This underscores the significance of modal number selection.

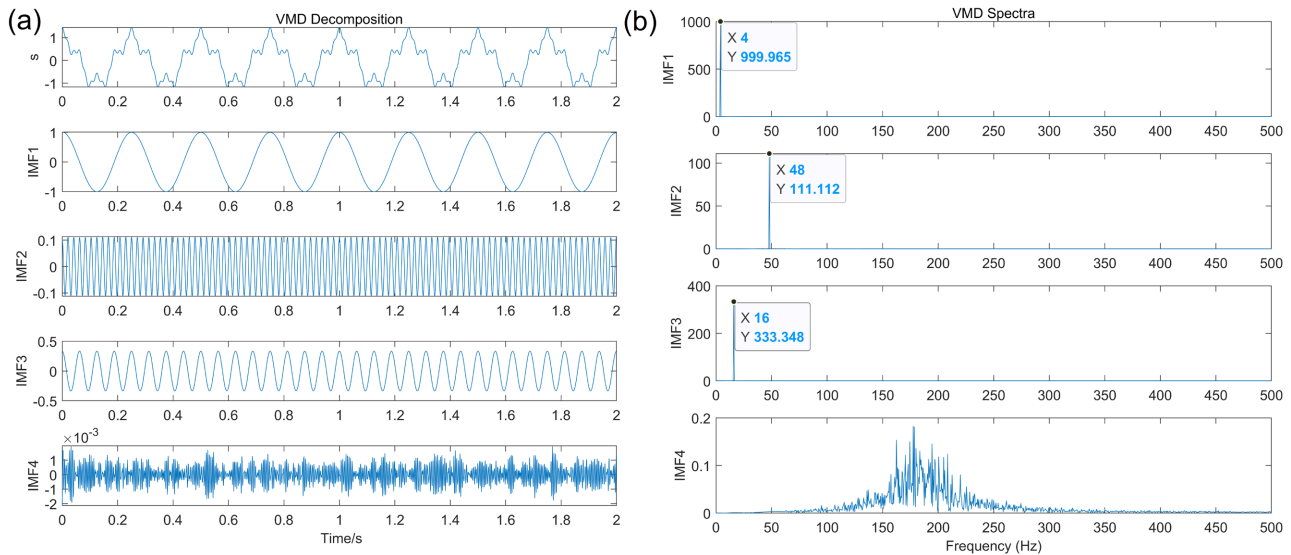


Figure 2. VMD of simulated signals: (a) time-domain decomposition of signals, and (b) spectra of decomposed components.

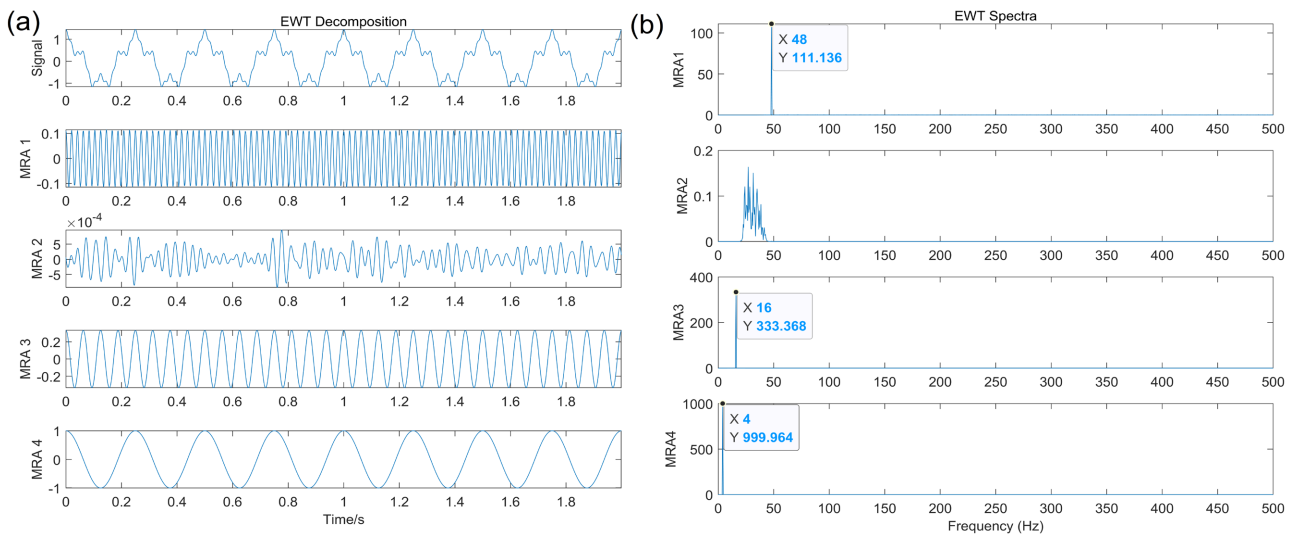


Figure 3. EWT decomposition of simulated signals: (a) time-domain decomposition of signals, and (b) spectra of decomposed components.

In general, predicting the number of modes N for a signal segment without prior information can be challenging. Hence, Gilles proposed a straightforward N -value estimation method: detecting M maximum points in the Fourier spectrum of the signal and assembling them into a set $\{M_i\}$. These M_i values are then arranged in descending order within the set, yielding $M_1 > M_2 > M_3 > \dots > M_M$. Setting a threshold at $M_M + \beta (M_1 - M_M)$, where β represents the relative ampli-

tude ratio, the number of extreme points surpassing this threshold plus 1 corresponds to the value of N .

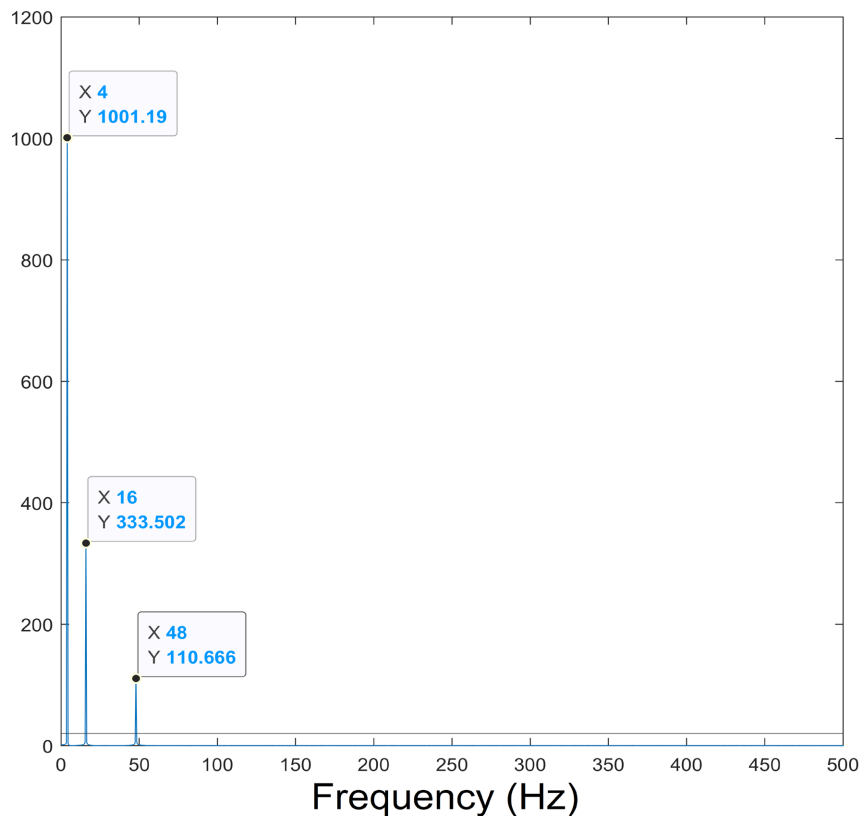


Figure 4. Gilles principle for determining frequency band division numbers.

Following this principle, the spectrum and the calculated threshold are depicted in **Figure 4** (where β is $1/50$). It is evident that the maximum value obtained by Gilles's method is 3, corresponding to a frequency band division of 4, which aligns with the frequency band division derived from the method discussed in this article.

4. Experimental Analysis

The structure of the EDM-3200 electric vibration system depicted in **Figure 5(a)** is illustrated in **Figure 5(b)**. The electric vibrator primarily comprises a magnetic circuit system and a motion system. The setup at the measurement site is illustrated in **Figure 6**, where microphone was positioned at each measurement point and connected to the MI-7008 signal processing unit. This unit was then linked to a computer for the collection and storage of noise signals at a sampling frequency of 51,200 Hz. This arrangement facilitated the capture of noise signals, enabling the determination of noise Sound Pressure Level (SPL) distribution based on the gathered data. To enhance the coherence, the research focuses on the noise signal generated by an electric vibrator operating at 1000 Hz with a magnitude of 5 g.

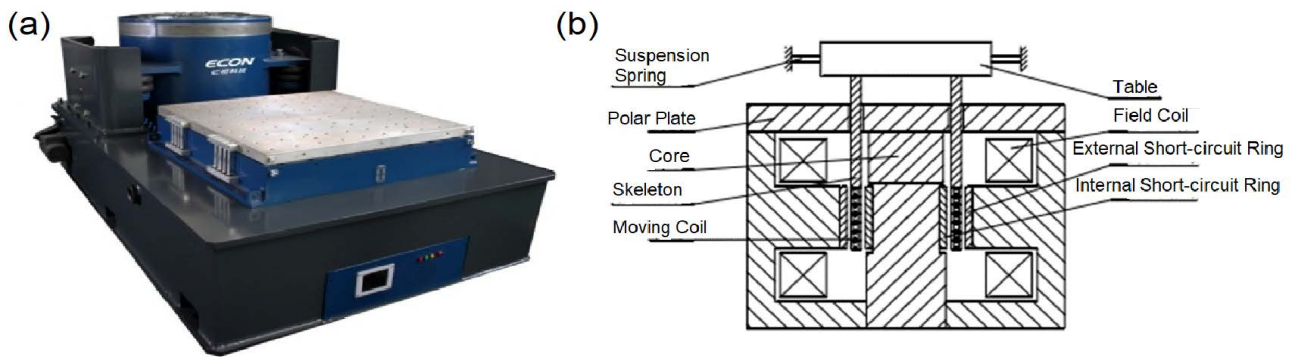


Figure 5. EDM-3200 electric vibrator: (a) the EDM-3200 electric vibration system, and (b) the structure of the vibrator.

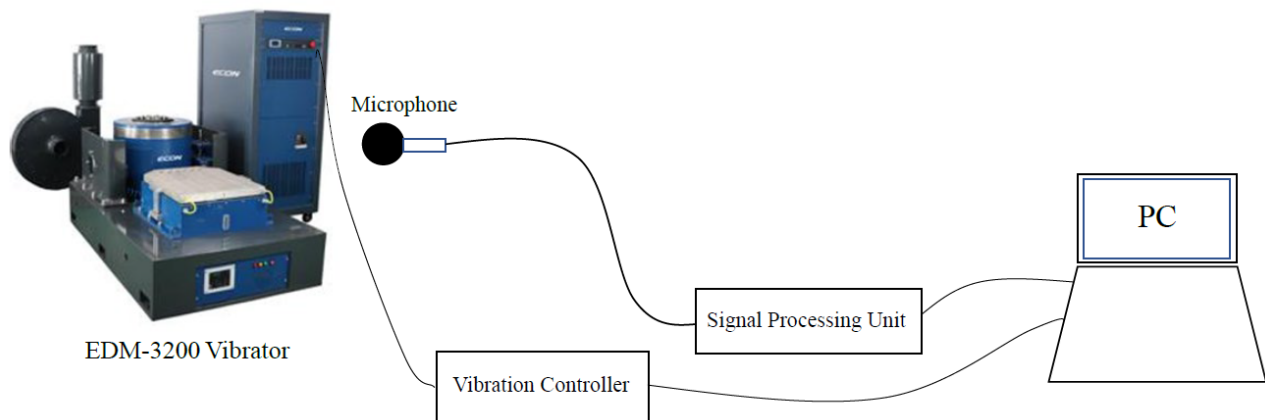


Figure 6. The setup at the measurement site.

The time-domain signal of the noise is depicted in **Figure 7**. Clearly, the signal comprises fundamental waves around 50 Hz and a series of high-frequency harmonics. Despite the chaotic nature, they exhibit certain periodicity and regularity.

The octave frequency spectrum of the noise at a specific measuring point on the electric vibrator is illustrated in **Figure 8**. Upon analysis of the octave frequency spectrum, it becomes apparent that the noise energy predominantly clusters around the 1000 Hz frequency range.

Similarly, **Figure 9** represent time-frequency map generated from the short-time Fourier transform. The map reveals that the most prominent noise occurs in the low-frequency range and around 1000 Hz at the onset of signal collection.

The VMD algorithm was utilized to decompose the noise signal, resulting in the extraction of IMFs and their corresponding frequency spectra, as illustrated in **Figure 10**. Based on the earlier mentioned judgment principle, when the modal number is set to 9, the residual of VMD decomposition is 0.057728. Increasing the modal number to 10 yields a residual of 0.056784, while further raising it to 11 results in a sharp drop to 0.042278. Consequently, the mode decomposition number indicating stability is 10. For EWT, the mode number

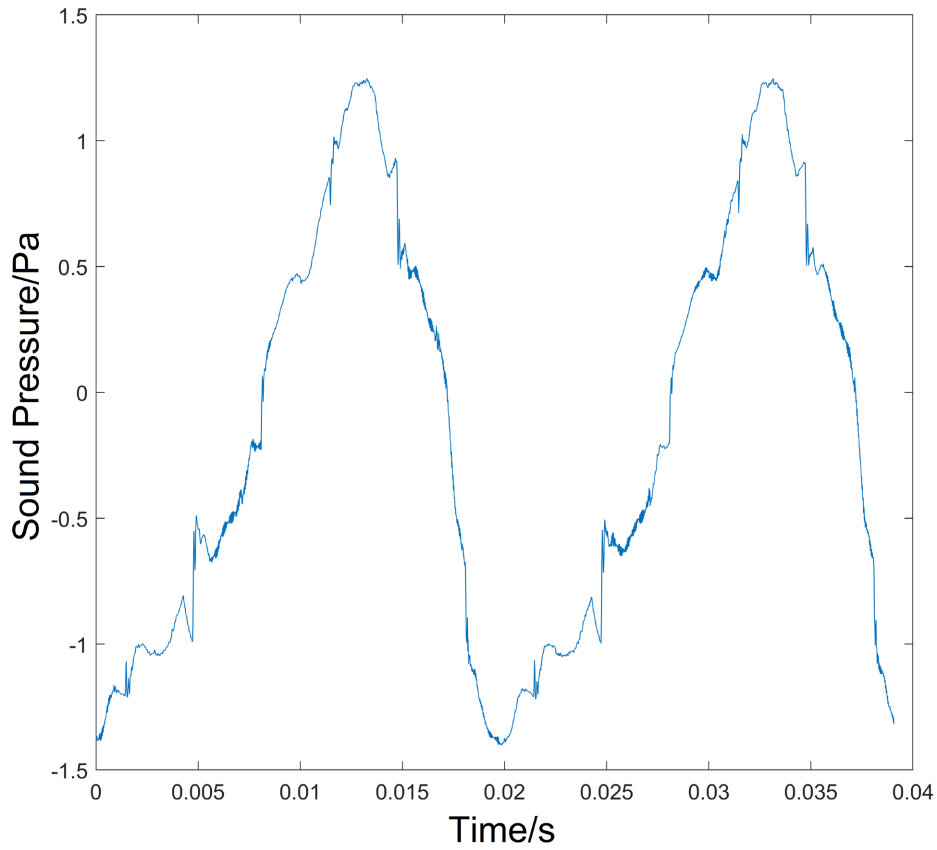


Figure 7. The signal of noise under the working condition: sinusoidal 1000 Hz at 5 g.

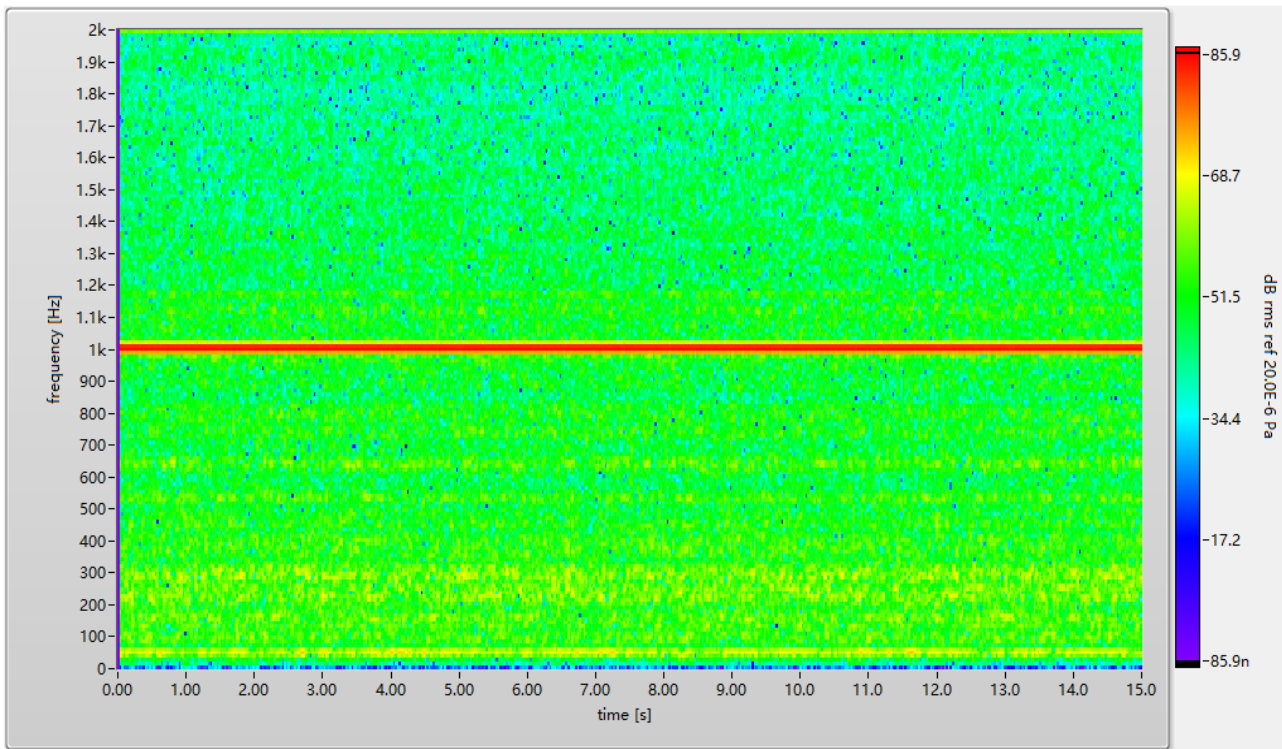


Figure 8. The octave spectra of noise under the working condition: sinusoidal 1000 Hz at 5 g.

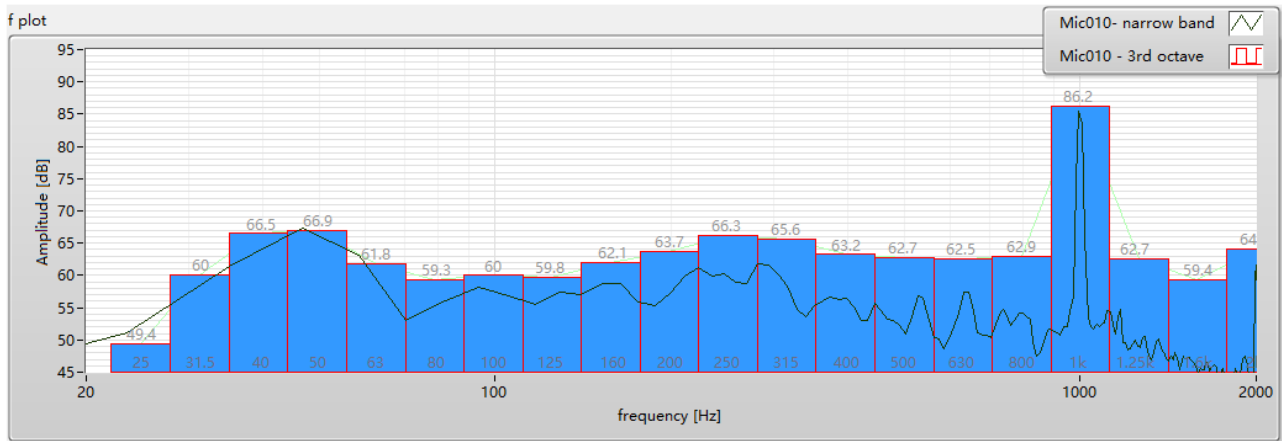


Figure 9. Time-frequency characteristics of noise under the working condition: sinusoidal 1000 Hz at 5 g.

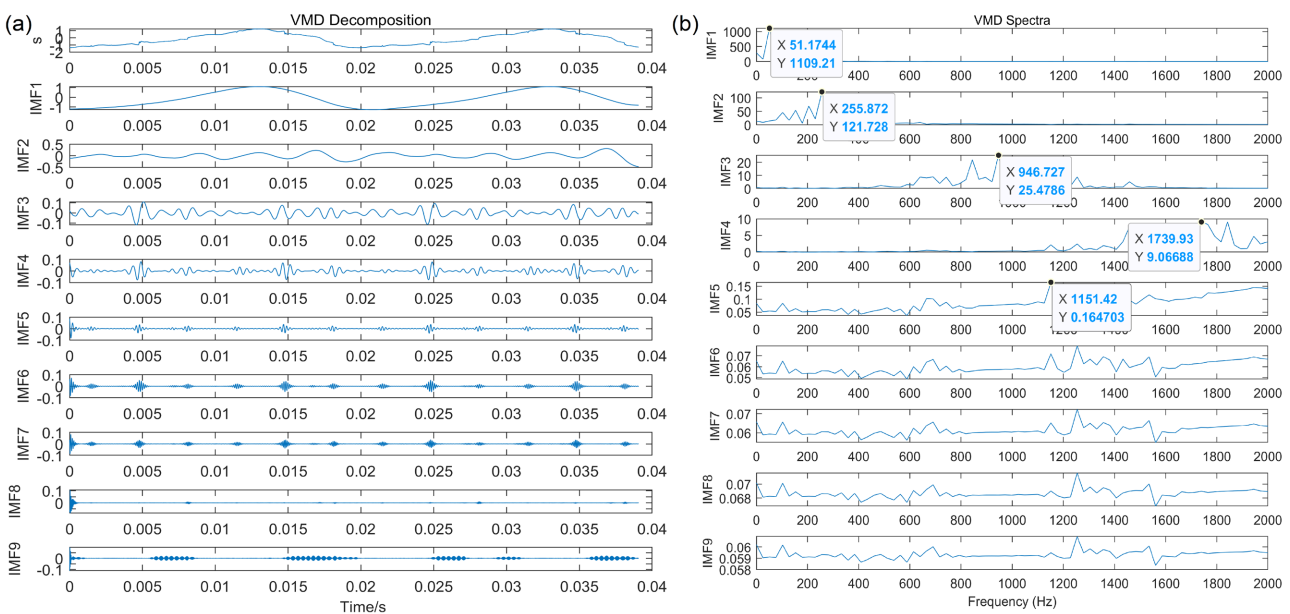


Figure 10. VMD of noise signals: (a) time-domain decomposition of signals, and (b) spectra of decomposed components.

determined by VMD is 9, with the corresponding frequency band division number set to 9. Among these decomposed components, low-frequency signals exhibit the largest proportion and pertain to the fundamental frequency signal. However, the second largest proportion occurs near 250 Hz. The obtained result is not in line with the conclusions drawn from the preceding analysis.

Hence, we utilize the EWT with a frequency band division of 9 to decompose the reconstructed signal after VMD, resulting in the extraction of Multi-resolution Analyses (MRAs) and their corresponding frequency spectrum, as illustrated in **Figure 11**. From the figure, it is evident that EWT can not only decompose low-frequency signals but also effectively separate the intermediate frequency signals (1000 Hz) corresponding to the signal octave spectrum and time-frequency map. This demonstrates both the advantages of EWT in alleviating mode aliasing and the result of EWT processing signals reconstructed after VMD decom-

position, thereby additionally preventing the generation of interference terms.

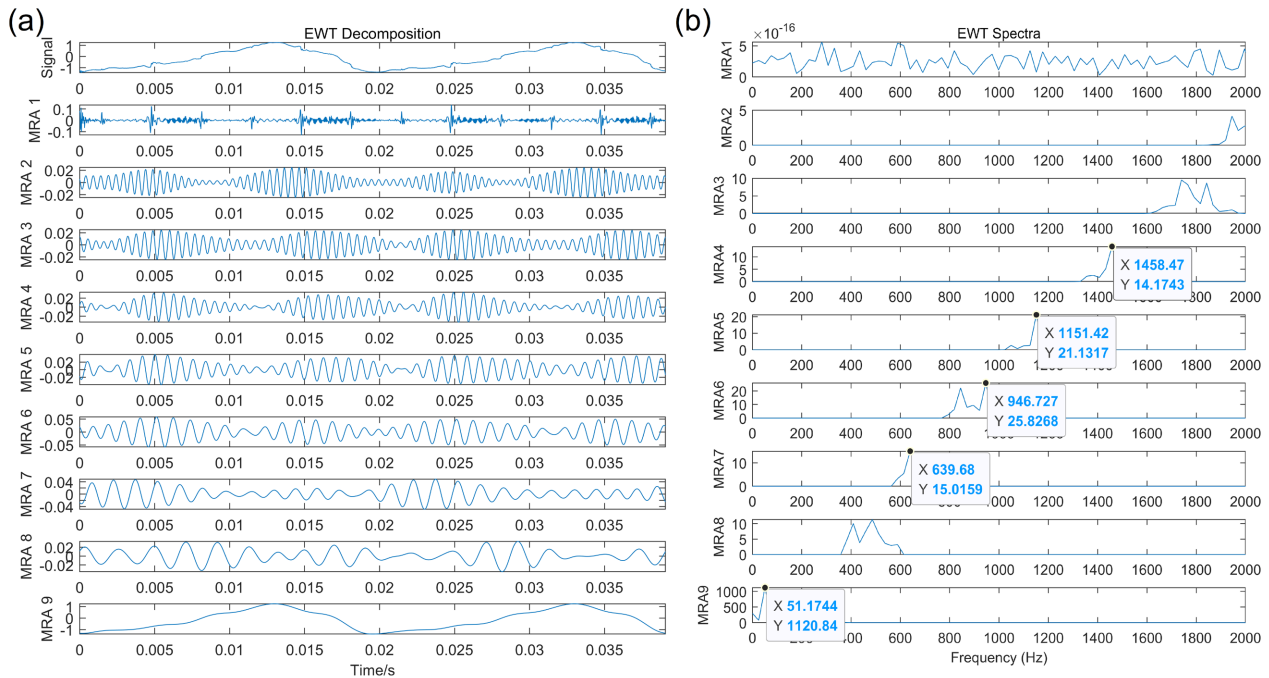


Figure 11. EWT decomposition of noise signals: (a) time-domain decomposition of signals, and (b) spectra of decomposed components.

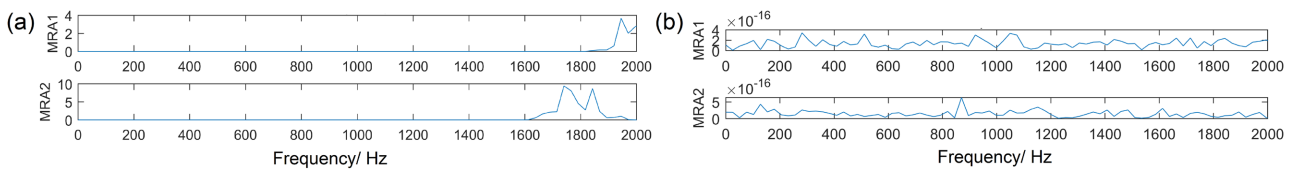


Figure 12. Spectra of the two MRAs with the smallest amplitudes: when the number of frequency band division is set to 8, and (b) when the number of frequency band division is set to 10.

Moreover, to validate the significance of frequency band division for the EWT method, we processed the signal using EWT algorithms with $N = 8$ and $N = 10$, respectively. **Figure 12(a)** and **Figure 12(b)** show the spectra of the two MRAs with the smallest amplitudes for $N = 8$ and $N = 10$, respectively. Based on the decomposition outcomes, it is evident that if the frequency band division of the EWT method is less than the correct division, it fails to completely separate the signals of all components. Conversely, when the number of frequency bands exceeds the correct number, it generates extra sub-signals, reducing the singularity of signal decomposition mode.

5. Conclusion

This article tackles the challenges posed by VMD mode aliasing and EWT’s limited adaptability in partitioning frequency bands during signal decomposition. Building upon these two algorithms, an enhanced approach that integrates VMD into the frequency band division principle of EWT was proposed. This method

initially decomposes the signal through VMD, determines the number of modes based on residuals, and subsequently reconstructs the signal after VMD decomposition using EWT decomposition. The results demonstrate that the proposed method effectively leverages the advantages of both VMD and EWT, enabling efficient decomposition of the noise signal generated by the electric vibrator. Furthermore, this method mitigates the drawback of the EWT method's lack of a basis for frequency band division. In comparison to the VMD method, this approach accurately decomposes noise signals into corresponding frequency components.

Conflicts of Interest

The authors declare no conflicts of interest regarding the publication of this paper.

References

- [1] Hermawanto, D., Ishikawa, K., Yatabe, K. and Oikawa, Y. (2023) Determination of Microphone Acoustic Center from Sound Field Projection Measured by Optical Interferometry. *The Journal of the Acoustical Society of America*, **153**, 1138-1146. <https://doi.org/10.1121/10.0017246>
- [2] Fiebig, W. and Dąbrowski, D. (2020) Use of Acoustic Camera for Noise Sources Localization and Noise Reduction in the Industrial Plant. *Archives of Acoustics*, **45**, 111-117. <https://doi.org/10.24425/aoa.2020.132487>
- [3] Rabaoui, A., Lachiri, Z. and Ellouze, N. (2004) Automatic Environmental Noise Recognition. *IEEE International Conference on Industrial Technology*, Hammamet, 8-10 December 2004, 1670-1675.
- [4] Potter, R.K., Kopp, G. and Green, H.C. (1947) Visible Speech. Van Nostrand, New York.
- [5] Mallat, S.G. and Zhang, Z. (1993) Matching Pursuits with Time-Frequency Dictionaries. *IEEE Transactions on Signal Processing*, **41**, 3397-3415. <https://doi.org/10.1109/78.258082>
- [6] Huang, N.E., Shen, Z., Long, S.R., et al. (1998) The Empirical Mode Decomposition and the Hilbert Spectrum for Nonlinear and Non-Stationary Time Series Analysis. *Proceedings of the Royal Society of London. Series A: Mathematical, Physical and Engineering Sciences*, **454**, 903-995. <https://doi.org/10.1098/rspa.1998.0193>
- [7] Huang, N.E., Shen, Z. and Long, S.R. (1999) A New View of Nonlinear Water Waves: The Hilbert Spectrum. *Annual Review of Fluid Mechanics*, **31**, 417-457. <https://doi.org/10.1146/annurev.fluid.31.1.417>
- [8] Dragomiretskiy, K. and Zosso, D. (2013) Variational Mode Decomposition. *IEEE Transactions on Signal Processing*, **62**, 531-544. <https://doi.org/10.1109/TSP.2013.2288675>
- [9] Gilles, J. (2013) Empirical Wavelet Transform. *IEEE Transactions on Signal Processing*, **61**, 3999-4010. <https://doi.org/10.1109/TSP.2013.2265222>
- [10] Gan, M., Pan, H., Chen, Y. and Pan, S. (2021) Application of the Variational Mode Decomposition (VMD) Method to River Tides. *Estuarine, Coastal and Shelf Science*, **261**, Article ID: 107570. <https://doi.org/10.1016/j.ecss.2021.107570>
- [11] Zhang, S., Wang, Y., He, S. and Jiang, Z. (2016) Bearing Fault Diagnosis Based on Vari-

ational Mode Decomposition and Total Variation Denoising. *Measurement Science and Technology*, **27**, Article ID: 075101.

<https://doi.org/10.1088/0957-0233/27/7/075101>

- [12] Wang, D., Zhao, Y., Yi, C., Tsui, K.L. and Lin, J. (2018) Sparsity Guided Empirical Wavelet Transform for Fault Diagnosis of Rolling Element Bearings. *Mechanical Systems and Signal Processing*, **101**, 292-308.

<https://doi.org/10.1016/j.ymssp.2017.08.038>

- [13] Wardana, A.N. (2016) A Comparative Study of EMD, EWT and VMD for Detecting the Oscillation in Control Loop. *International Seminar on Application for Technology of Information and Communication*, Semarang, 5-6 August 2016, 58-63.